SYSTEM SAFETY: HUMAN - TECHNICAL FACILITY – ENVIRONMENT
7(1), 2025, pp. 315-325

MICROSTRUCTURAL AND MAGNETIC RESPONSE OF AUSTENITIC STAINLESS STEELS TO PLASTIC DEFORMATION

DOI: 10.2478/czoto-2025-0030
Received: 10/11/2025
Accepted: 10/12/2025

Martin Slezák[1] – *orcid id: 0009-0008-3181-0862, e-mail: martin.slezak@fstroj.uniza.sk*
Peter Palček[1] – *orcid id: 0000-0001-7902-2007, e-mail: peter.palcek@fstroj.uniza.sk*
Kamila Hrabovská[2] – *orcid id: 0000-0003-4563-6558, e-mail: kamila.hrabovska@vsb.cz*
Ondřej Životský[2] – *orcid id: 0000-0002-5715-468X, e-mail: ondrej.zivotsky@vsb.cz*
Milan Uhríčik[1] – *orcid id: 0000-0002-2782-5876, e-mail: milan.uhricik@fstroj.uniza.sk*
Melisa Šnircová[1] – *orcid id: 0009-0008-0014-713X, e-mail: melisa.snircova@fstroj.uniza.sk*
[1]Department of materials engineering, University of Žilina, Univerzitná 8215/1, Žilina, **Slovakia**
[2]Department of physics, VSB - Technical University of Ostrava, 17. listopadu 2172/15, Ostrava, **Czechia**

Abstract: The study investigates the influence of pressure-induced plastic deformation on the microstructural evolution, microhardness, and magnetic behavior of AISI 304 and AISI 316L austenitic stainless steels. Samples were subjected to different levels of compressive deformation and subsequently analyzed using optical microscopy, microhardness testing, and vibrating sample magnetometry (VSM). The microstructure after solution annealing consisted of polyhedral austenitic grains with numerous annealing twins, while after deformation, distinct signs of plastic strain were observed within individual grains. The microhardness measured perpendicular to the loading direction increased with the degree of deformation, reaching the highest values in the core of the samples, which confirms the non-uniform distribution of plastic deformation. Magnetic measurements revealed a noticeable increase in both saturation and remanent magnetization after plastic deformation, confirming the presence of deformation-induced α′-martensite. The coercive field decreased for AISI 304 but slightly increased for AISI 316L. The results demonstrate a clear correlation between mechanical strengthening and the magnetic response of austenitic steels subjected to plastic deformation.
Keywords: Austenitic stainless steel, plastic deformation, microhardness, magnetic properties, α′-martensite

1. INTRODUCTION

Austenitic stainless steels are among the most commonly utilized materials in industrial applications due to their excellent corrosion resistance, biocompatibility, and paramagnetic behavior in the annealed condition, combined with a relatively low production cost compared to alternative alloys (de Araújo Junior et al., 2019; Godec., 2020). Despite these advantages, their practical use is limited by their low hardness, moderate strength, and susceptibility to wear. The mechanical strength and hardness can

be improved through cold working. However, this process significantly changes the internal properties of austenitic stainless steel. During plastic deformation, is α′-martensite formed within the microstructure, leading to transformation from paramagnetic to ferromagnetic (Frizt, 2020; Cisquini, 2019). It has been reported that the susceptibility of austenite to martensite transformation is influenced by its chemical composition, stacking fault energy, and temperature. Moreover, chromium can either increase or decrease the stacking fault energy depending on the nickel content in the alloy. This relationship is crucial because the stacking fault energy determines the dominant deformation mechanisms in austenitic steels. Lower stacking fault energy promotes the formation of deformation twins and facilitates the nucleation of α′-martensite during plastic deformation, while higher values favor dislocation slip and suppress the martensitic transformation (Curtze et al., 2011).
This study investigates the variation in structural and physical properties of two austenitic stainless steel subjected to plastic deformation.

2. MATERIALS AND METHODS

Austenitic stainless steels AISI 304 and AISI 316L were used for this experiment. The material was supplied in the form of circular bars with a length of 3000 mm and a diameter of 12 mm. Cylindrical specimens with a height of 15 mm and a diameter of 12 mm were mechanically cut from these bars. A chemical analysis was subsequently performed on the prepared samples using an emission spark spectrometer SPECTROMAXx in order to verify their chemical composition. The results of these analyses are presented in Table 1. In order to remove internal stresses and obtain the initial reference state before the experimental procedures, a solution annealing (SA) treatment was carried out on the austenitic stainless steels. The heat treatment was performed at the Rübig SK company. Before the process, the specimens were cleaned with isopropyl alcohol and subsequently placed into the furnace. Solution annealing was conducted at a temperature of 1030 °C for 30 minutes under a vacuum atmosphere. After the holding time, the samples were rapidly cooled using gaseous nitrogen, ensuring the retention of the fully austenitic microstructure.

Table 1
Elemental composition of the investigated materials

Type of steel	**The concentration of chemical elements [wt. %]**								
	C	**Cr**	**Ni**	**Mo**	**Mn**	**Si**	**S**	**P**	**Fe**
AISI 304	0.02	18.87	8.18	0.40	1.35	0.40	0.03	0.03	balance
1.4301	≤0.07	17.5-19.5	8.0-10.5	-	≤2.00	≤1.00	≤0.015	≤0.045	balance
AISI 316L	0.02	17.02	10.23	2.11	1.48	0.38	0.02	0.04	balance
1.4404	≤0.03	16.5-18.5	10.0-13.0	2.00-2.50	≤2.00	≤1.00	≤0.015	≤0.045	balance

After the solution annealing treatment, the main part of the experiment was initiated. In this stage, the specimens were subjected to plastic deformation by compressive loading. The applied load ranged from 5 to 25 tons, with each subsequent specimen deformed

under an incrementally higher-pressure step of 5 tons. For each steel grade, a total of six samples were prepared - one solution annealed reference sample and five samples with different levels of deformation (Fig. 1). The specimen dimensions after deformation, as well as the calculated percentage reduction in height, are presented in Table 2. To ensure a reliable characterization of the microstructure, all specimens in their respective conditions underwent a standard metallographic preparation. The procedure involved sequential grinding, fine polishing, and subsequent chemical etching. The etching process was carried out using the Kallings 2 reagent, consisting of a mixture of 5 g $CuCl_2$, 100 ml HCl, and 100 ml ethanol, with an average etching duration of approximately 15 seconds. Following the metallographic preparation, the microstructural evaluation was conducted using a NEOPHOT 32 optical microscope. The microstructure was captured and processed in the NIS Elements 4 software at a magnification of 400×. In addition, Vickers microhardness testing was performed employing the static indentation method on a Zwick/Roell ZHμ tester under a load applied (HV 0.5) for 10 seconds at a room temperature of about ± 20 °C. The schematic representation of the metallographic sampling and subsequent microhardness measurement is shown in Figure 2.

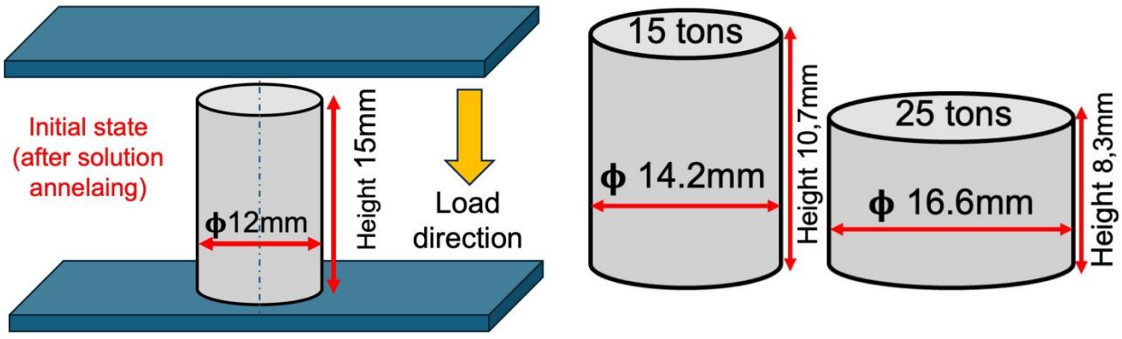

Fig. 1. Geometry of the cylindrical specimens before and after plastic deformation; a) reference state after solution annealing and before deformation, b) deformed states corresponding to different applied loads

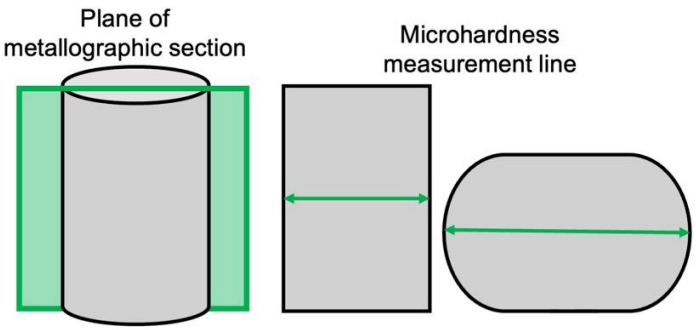

Fig. 2. Schematic illustration of the sampling location and microhardness measurement positions

Following the microstructural analysis, microhardness measurements were performed to evaluate the local strengthening effect induced by plastic deformation. The hardness testing was conducted prior to the magnetic characterization. Subsequently, magnetic measurements were carried out at the Department of Physics, VŠB – Technical University of Ostrava. The specimens for bulk magnetization testing were prepared by electroerosive cutting to ensure precise geometry and to avoid thermal influence on the microstructure.

The final samples had a cylindrical shape with a diameter of 4 mm and a thickness of 2 mm. The magnetization curves were recorded at room temperature using a vibrating sample magnetometer (VSM, MicroSense EZ9) under an applied magnetic field of ±1600 kA/m.

Table 2
Dimensions and deformation levels of AISI 304 and AISI 316L samples

AISI 304				AISI 316L			
Sample No.	**Applied load [t]**	**Height after deformation [mm]**	**Deformation [%]**	**Sample No.**	**Applied load [t]**	**Height after deformation [mm]**	**Deformation [%]**
1	0	15.0	0	**1**	0	15.0	0
2	5	14.1	6.0	**2**	5	14.0	6.67
3	10	12.2	18.67	**3**	10	12.1	19.33
4	15	10.7	28.7	**4**	15	10.5	30
5	20	9.3	38.0	**5**	20	9.0	40
6	25	8.3	44.67	**6**	25	7.9	47.33

3. RESULTS AND DISCUSSION

The following section presents and discusses the experimental findings obtained from microstructural observations, microhardness testing, and magnetic measurements. Particular attention is devoted to the correlation between the degree of plastic deformation and the resulting changes in the structural and magnetic properties of the investigated austenitic stainless steels.

3.1 Microstructural analysis

After solution annealing, the microstructures of AISI 304 and AISI 316L steels consisted of polyhedral austenitic grains with a variable grain size distribution. In both materials, numerous annealing twins (indicated by red arrows) were clearly distinguishable throughout the matrix. No regions containing δ-ferrite were observed, confirming the fully austenitic character of the microstructure after solution annealing. In both cases, non-metallic inclusions with an elongated morphology were also detected. This condition is therefore considered the reference state for subsequent comparisons. Representative microstructures are shown in Figures 3a and 3b.

a) b)

Fig. 3. Microstructure of austenitic stainless steel; a) AISI 304, b) AISI 316L, etch.

The elongated non-metallic inclusions detected in both steels were thoroughly investigated using SEM and EDX mapping and were identified as manganese sulfides (MnS) Fig.4. MnS inclusions often form during casting and solidification due to the low solubility of sulfur in the iron matrix and the affinity of manganese for sulfur. MnS inclusions are well known to act as preferential sites for localized corrosion initiation in austenitic stainless steels. In particular, recent work has demonstrated that pits frequently nucleate at MnS inclusions, and their dissolution can trigger events such as intergranular corrosion and depassivation of sensitized material.

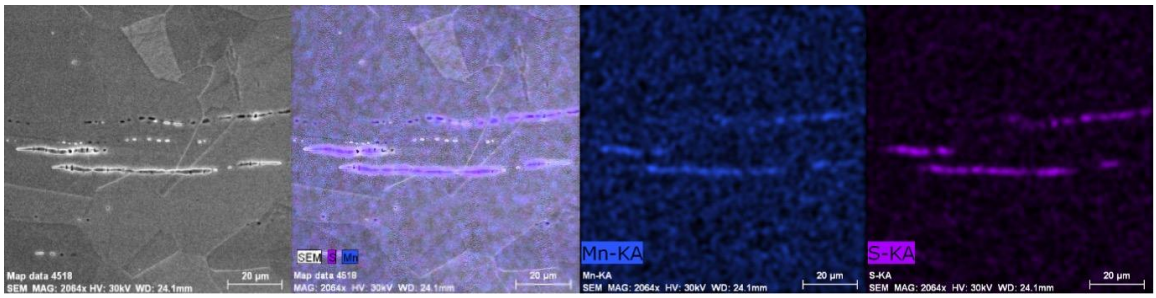

Fig. 4. SEM detected manganese sulfides

After plastic deformation, noticeable microstructural changes were observed in both experimental steels (Fig. 5). The micrographs show progressive deformation of individual austenitic grains, with the intensity of this effect increasing with the degree of deformation.

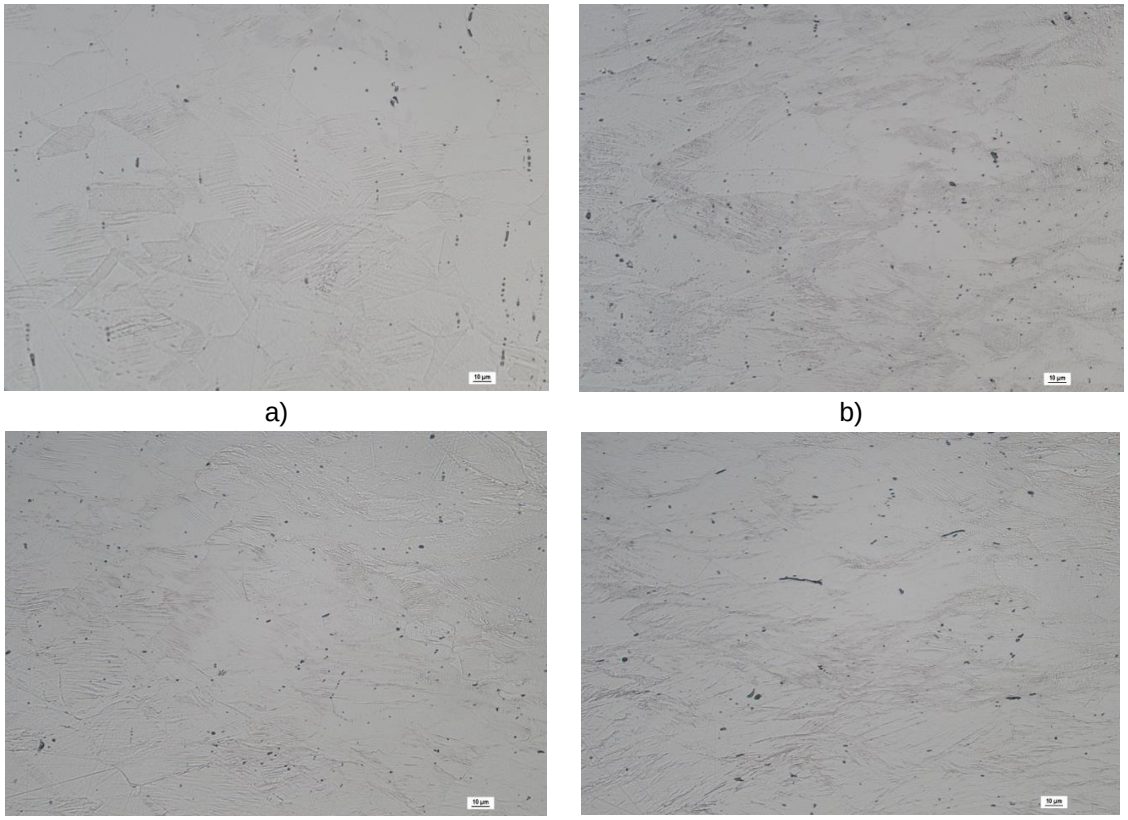

a) b)

c) d)

Fig. 5. Examples of microstructure of austenitic stainless steel after plastic deformation; a) AISI 304 10t, b) AISI 304 25t, c) AISI 316L 15t, d) AISI 316L 25t, magnification 400x, etch.

The annealing twins, which were clearly distinguishable in the solution-annealed condition, are now partially fragmented or bent, and their continuity is disrupted. Non-metallic manganese sulfide (MnS) inclusions are no longer aligned or uniformly distributed; instead, they appear in a more random orientation within the deformed matrix. Importantly, at higher deformation levels the onset of strain-induced α′-martensite formation is evident: shear bands and intersecting twin- and slip-band networks act as preferential nucleation sites for the transformation γ-austenite → α′-martensite (Sohrabi et al., 2020). This development underpins the significant work-hardening observed in the sections that follow, specifically in the hardness and magnetic response sections.

3.2 Evaluation of microhardness

Figure 6 and Table 3 summarize the microhardness results obtained for AISI 304 after plastic deformation under various compressive loads. The lowest microhardness values were recorded in the solution-annealed condition, showing a uniform distribution of approximately 146 HV0.5. With increasing deformation, the microhardness of the steel rose significantly, indicating pronounced strain hardening. The highest microhardness values, reaching up to 409 HV0.5, were measured in the sample deformed under 25 tons.

Table 3
Minimum, maximum and average values measured on AISI 304 samples

AISI 304	minimum	maximum	average
Solution annealing	143	155	146
10t	263	345	310
15t	322	369	354
25t	307	409	370

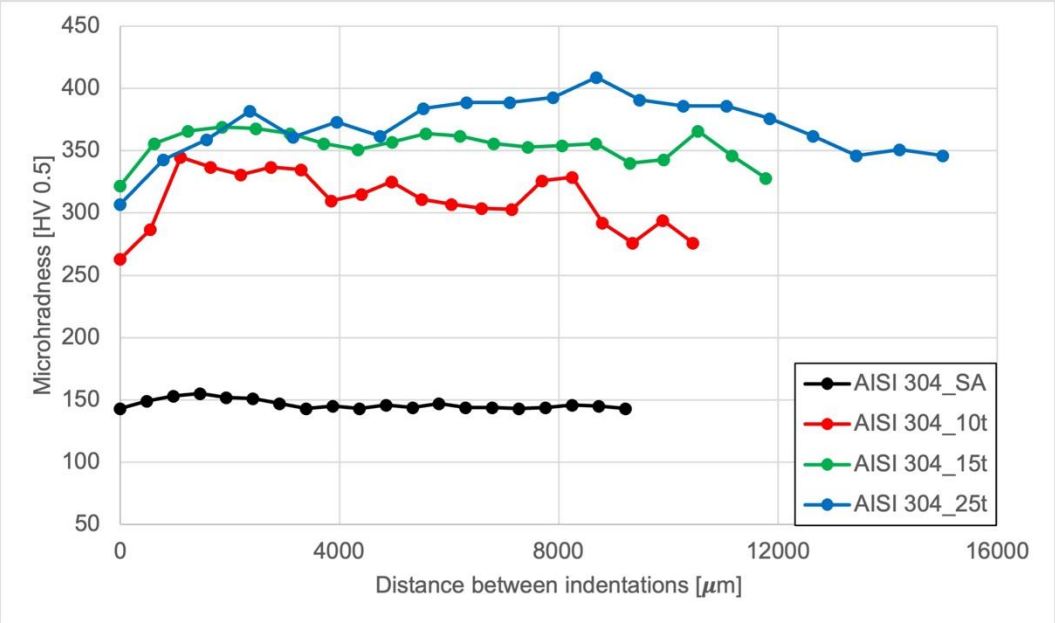

Fig. 6 Microhardness profile of austenitic stainless steel AISI 304

The hardness distribution across the specimen revealed a non-uniform pattern, with higher values measured in the central region compared to the edges. This gradient confirms that the plastic strain was not evenly distributed throughout the volume, which is

consistent with the deformation mode typical of compression tests. The observed hardening is attributed to two concurrent mechanisms: the accumulation of dislocations within the austenitic matrix and the formation of deformation-induced α′-martensite. As reported by (Talonen and Hänninen, 2007; Sohrabi et al., 2020), the progressive increase in dislocation density during cold working enhances lattice friction stress, while the partial transformation of metastable austenite (γ) to α′-martensite provides an additional strengthening contribution.

The results of microhardness measurements for AISI 316L after plastic deformation are shown in Figure 7 and summarized in Table 4. The lowest microhardness values were measured in the solution-annealed condition, with an average of 135 HV0.5. With increasing deformation, the microhardness of the material gradually increased, reaching a maximum of 414 HV0.5 in the sample deformed under a load of 25 tons. The hardness distribution across the specimen revealed a non-uniform profile similar to that observed for AISI 304. The highest microhardness values were recorded in the central region of the samples, while slightly lower values were measured near the edges. This confirms that the plastic deformation was not evenly distributed throughout the entire volume of the specimen. The gradual increase in hardness with higher deformation levels indicates a clear work-hardening effect caused by the applied compressive strain.

Table 4
Minimum, maximum and averages values measured on AISI 316L samples

AISI 316L	minimum	maximum	average
Solution annealing	129	139	135
10t	263	321	298
15t	289	375	337
25t	283	414	362

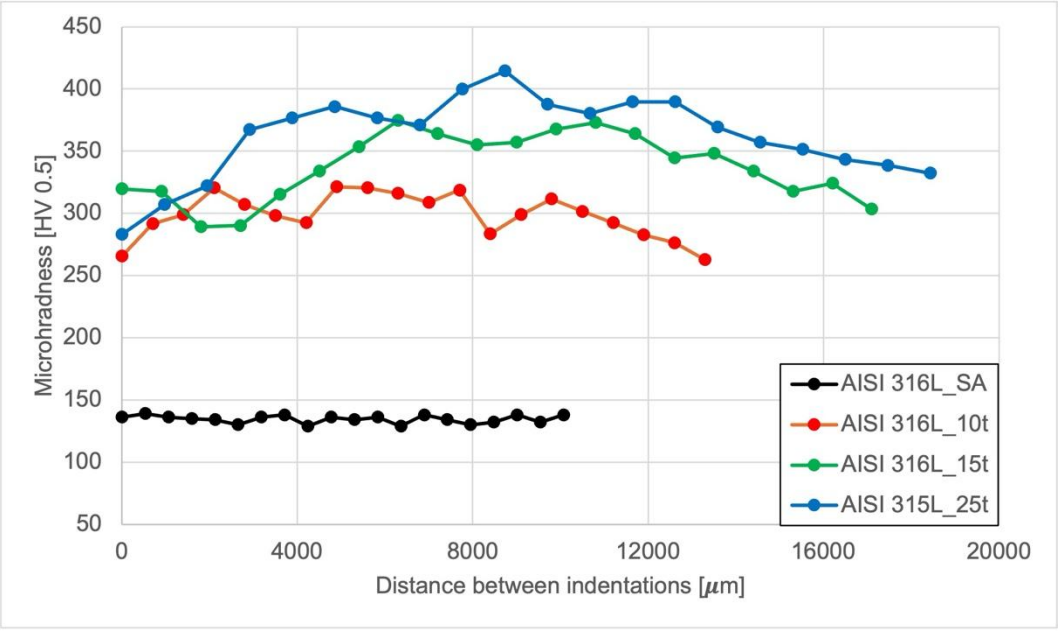

Fig. 7 Microhardness profile of austenitic stainless steel AISI 316L

In summary, the results of the microhardness measurements demonstrated a clear increase in hardness with rising levels of plastic deformation for both investigated steels.

The most pronounced hardening effect was observed in AISI 304, while AISI 316L exhibited a slightly lower but still significant increase in hardness due to its higher austenite stability. The non-uniform hardness profiles across the specimen thickness confirmed that the applied compressive deformation was unevenly distributed within the material volume. Overall, the microhardness results correlate well with the observed microstructural changes, providing quantitative evidence of the progressive work-hardening induced by plastic deformation.

3.3 Magnetization

The mechanical strengthening observed through microhardness testing suggests substantial structural rearrangements within the austenitic matrix. To further characterize these changes, particularly the potential formation of deformation-induced α′-martensite, magnetic measurements were carried out on all specimens.

Figure 8 and Fig. 9 shows the hysteresis loops of the investigated steels after different levels of compressive deformation. The initial, solution-annealed samples displayed purely paramagnetic behavior with negligible magnetization. With increasing plastic deformation, a distinct ferromagnetic response gradually appeared, confirming the formation of deformation-induced α′-martensite.

For AISI 304, the increase in magnetization was significant, with saturation values reaching approximately 25 Am²/kg for the sample deformed under 25 tons. The coercive field (Hc) decreased from 13.97 to 4.97 kA/m, while the remanent magnetization (Mr) increased from 0.01 to 4.21 Am²/kg. This trend indicates that the α′-martensite formed progressively with strain and stabilized the ferromagnetic domains, while the decrease in coercivity suggests easier domain wall movement in the highly deformed microstructure.

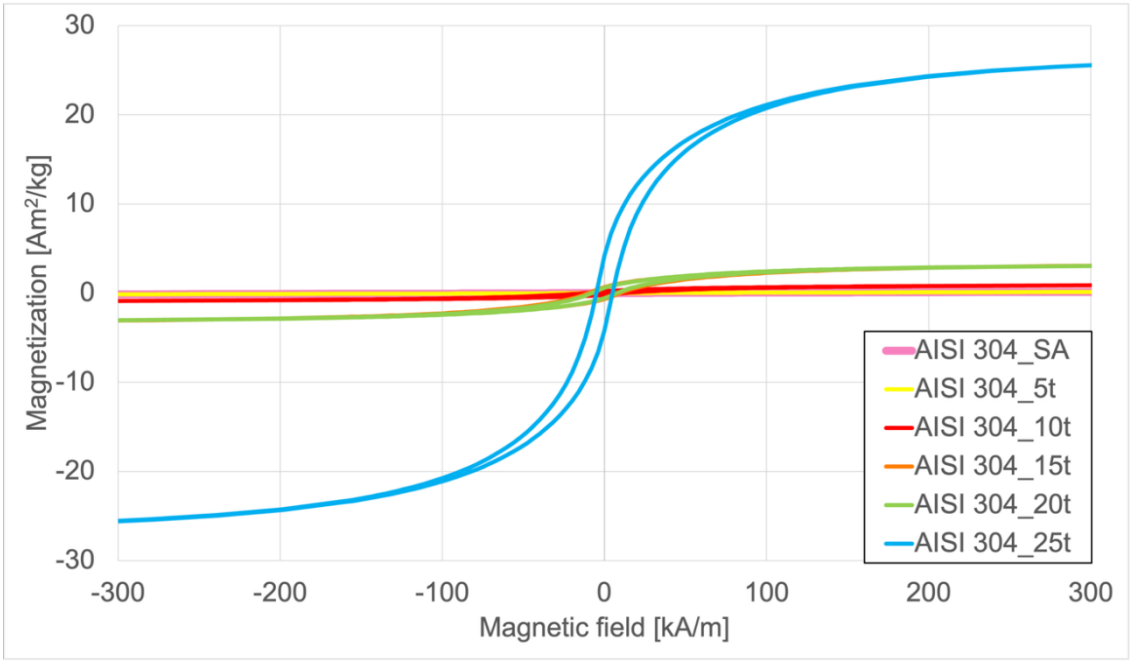

Fig. 8 Hysteresis loops of AISI 304 steel

In contrast, AISI 316L exhibited a much weaker magnetic response owing to its higher austenite stability. The maximum magnetization did not exceed 3 Am²/kg, and the overall Hc and Mr (Fig. 10) values remained significantly lower compared with AISI 304. However,

an unusual increase in coercivity at higher deformation levels (up to 11.6 kA/m) was recorded. Similar behavior was described by (Mitra et al., 2004) who attributed this behavior to the mechanism of ferromagnetism in the presence of low and high volume fractions of martensite. However, the authors obtained these results with AISI 304 steel.

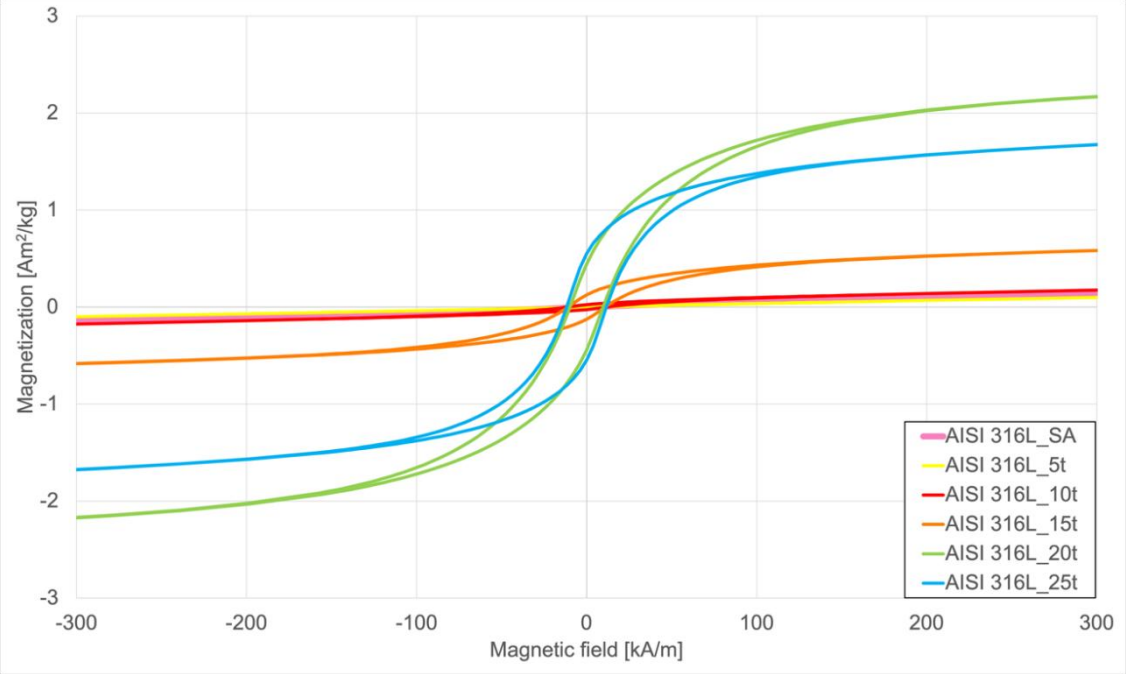

Fig. 9 Hysteresis loops of AISI 316L steel

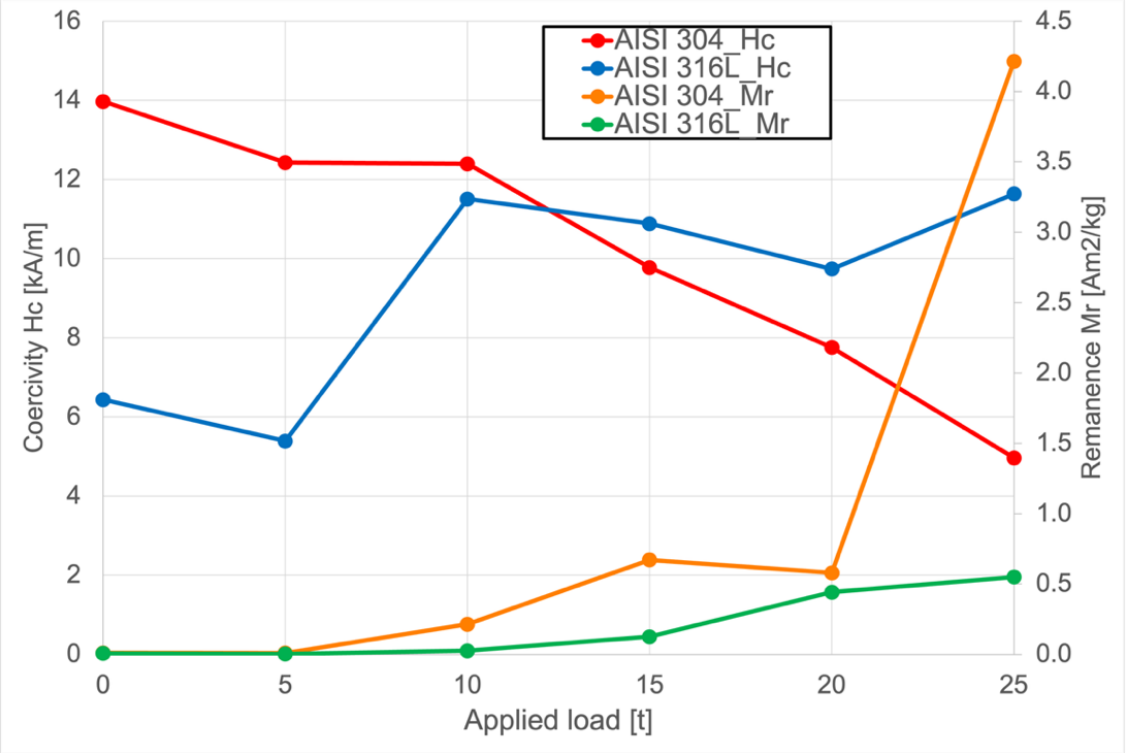

Fig. 10 Evolution of coercivity (Hc)and remanence (Mr) in AISI 304 and AISI 316L stainless steels with increasing plastic deformation

The slight decrease in Mr for AISI 304 between 15 t and 20 t can be attributed to local deformation inhomogeneity in the specimen volume, which is also supported by the microhardness results showing a non-uniform strain distribution.
The observed increase in magnetic response with plastic deformation may have practical implications for industrial applications that require monitoring of mechanical loading or structural integrity. Since the formation of deformation-induced α′-martensite directly affects magnetization, the measured magnetic parameters could serve as a non-destructive indicator of prior deformation, strain accumulation, or early-stage damage in austenitic stainless steel components. This correlation opens possibilities for using magnetic measurements as a diagnostic tool in quality control, life assessment of mechanically loaded parts, and real-time monitoring of components operating in demanding environments.

4. CONCLUSION

Based on the experimental results and analyses, the following conclusions were drawn the influence of plastic deformation on the structural, mechanical, and magnetic behavior of the investigated steels:

- The microstructural analysis revealed that both AISI 304 and AISI 316L possessed a fully austenitic structure after solution annealing, composed of polyhedral grains with numerous annealing twins. With increasing compressive deformation, a gradual distortion of individual grains was observed, indicating the onset of strain localization within the austenitic matrix.
- The microhardness of both steels increased with the degree of plastic deformation, confirming a clear work-hardening effect. The most pronounced increase was observed in AISI 304, while AISI 316L showed a slightly lower rise due to its higher austenite stability.
- Magnetic measurements confirmed the formation of ferromagnetic α′-martensite during deformation. The magnetization and remanence increased progressively with strain, with AISI 304 showing a much stronger magnetic response compared to AISI 316L. The coercive field decreased in AISI 304 but slightly increased in AISI 316L, reflecting different martensite distributions and domain wall behavior.

Both microhardness profiles and magnetic results indicated that the plastic deformation was not uniformly distributed throughout the specimen volume. The core regions exhibited higher strain and property changes than the edges, confirming the non-homogeneous character of the applied compressive deformation.

ACKNOWLEDGEMENTS

Funded by the EU NextGenerationEU through the Recovery and Resilience Plan for Slovakia under the project No. 09I03-03-V05-00002. The research was also supported by the Scientific Grant Agency of the Ministry of Education of the Slovak Republic, KEGA 016ŽU-4/2023. The research was supported by Rübig SK, where solution annealing of AISI 304 and AISI 316Laustenitic steel samples was carried out.

REFERENCES

Cisquini, P., Ramos, S. V., Viana, P. R. P., de Freitas Cunha Lins, V., Franco Jr, A. R., Vieira, E. A. 2019, *Effect of the roughness produced by plasma nitrocarburizing on corrosion resistance*

of AISI 304 austenitic stainless steel, Journal of Materials Research and Technology, 8 (2), 1897-1906, DOI: 10.1016/j.jmrt.2019.01.006

Curtze, S., Kuokkala, V. T., Oikari, A., Talonen, J., Hänninen, H., 2011, *Thermodynamic modeling of the stacking fault energy of austenitic steels*, Acta Materialia, 59 (3), 1068-1076, DOI: 10.1016/j.actamat.2010.10.037

de Araújo Junior, E., Bandeira, R. M., Manfrinato, M. D., Moreto, J. A., Borges, R., dos Santos Vales, S., Suzuki, P. A., Rossino, L. S. 2019. *Effect of ionic plasma nitriding process on the corrosion and micro-abrasive wear behavior of AISI 316L austenitic and AISI 470 super-ferritic stainless steels,* Journal of Materials Research and Technology, 8 (2), 2180-2191, DOI: https://doi.org/10.1016/j.jmrt.2019.02.006

Frizt, J. 2020. *Practical guidelines for the fabrication of austenitic stainless steels*, Encyklopedia. London. ISBN 978-1-907470-13-4.

Godec, M., Donik, Č., Kocijan, A., Podgornik, B., Balantič. D. A. S., 2020. *Effect of post-treated low-temperature plasma nitriding on the wear and corrosion resistance of 316L stainless steel manufactured by laser powder bed fusion*, Additive Manufacturing, 32, 1-9. DOI: 10.1016/j.addma.2019.101000

Mitra, A., De, P. K., Bhattacharya, D. K., Srivastava, P. K., Jiles, D., 2004, *Ferromagnetic properties of deformation-induced martensite transformation in AISI 304 stainless steel*, Metallurgical and Materials Transactions A, 35, 588 – 605, DOI: 10.1007/s11661-004-0371-6

Sohrabi, M. J., Naghizadeh, M., Mirzadeh, H., 2020, *Deformation-induced martensite in austenitic stainless steels: A review,* Archives of Civil and Mechanical Engineering, DOI: 10.1007/s43452-020-00130-1

Talonen, J., Hänninen, H., 2007, *Formation of shear bands and strain-induced martensite during plastic deformation of metastable austenitic stainless steels*, Acta Materialia, 55 (18), 6108 – 6118, DOI: 10.1016/j.actamat.2007.07.015